Available online at www.sciencedirect.com
ScienceDirect
Journal of Photochemistry and Photobiology A: Chemistry 185 (2007) 172–180
Journal of Photochemistry and Photobiology A:Chemistry
www.elsevier.com/locate/jphotochem

Photoinduced transformation of camptothecin in the presence of iron(III) ions

Dana Dvoranová, Vlasta Brezová*, Marian Valko, Andrej Staško

Department of Physical Chemistry, Faculty of Chemical and Food Technology, Slovak University of Technology in Bratislava, Radlinského 9, SK-812 37 Bratislava, Slovak Republic

Received 15 February 2006; received in revised form 1 June 2006; accepted 2 June 2006
Available online 25 July 2006

Abstract

To obtain the information on the photoactivated action of camptothecin (CPT) promoted by transition metals, CPT was UVA irradiated (λ = 365 nm) in dimethylsulfoxide (DMSO) solutions. Fe(III) ions present were efficiently reduced to Fe(II) under argon and also in the presence of oxygen. The photoinduced electron transfer under argon resulted into the generation of carbon-centered radicals identified by EPR spin trapping evidencing the cleavage of CPT skeleton. Whereas the absorption UV/vis experiments with equimolar ratio Fe(III):CPT excluded the formation of charge-transfer complexes, the fluorescence spectra of CPT in the presence of Fe(III) revealed a significant fluorescence quenching indicating the probability of physical association between Fe(III) and CPT species in DMSO solutions confirming Fe(III) involvement in the photoinduced transformation.

Keywords: Camptothecin; Electron transfer; EPR; Spin trapping technique; Iron(III) ions

1. Introduction

The anticancer drug camptothecin (CPT) is a plant alkaloid successfully applied in the treatment of gastric, rectum and bladder tumors [1–5]. Its structure (Scheme 1) comprises a quinoline ring system (**A** and **B**), a pyridone ring (**D**) and a terminal α-hydroxy-lactone ring (**E**), which is essential for its antitumor activity [5–10]. The intact hydroxy-lactone ring represents a structural requirement for the biological activity of CPT, as the biologically inactive, ring-opened carboxylate form of CPT, not only binds to human serum albumin lowering the effective concentration of CPT, but also exhibits toxic side effects [11]. Several clinically important water-soluble derivatives of CPT have been synthesized previously [12,13].

The camptothecin family of anticancer medicines has a unique mechanism of action directed to the inhibition of topoisomerase I (Topo I) [6–9]. It was previously shown that CPT inhibits Topo I via the formation of ternary complex, in which the biologically active lactone ring of CPT stabilizes an irreversible Topo I/DNA covalent complex [9].

Camptothecin molecule contains conjugated system of π-electrons representing a potential basis for UVA photoexcitation resulting in the reactive free radical species generation (e.g. ROS), which are responsible for light-mediated DNA cleavage [14–18]. Consequently, alternative mechanisms of DNA damage upon the simultaneous application of CPT, Topo I and UV radiation (λ = 365 nm) were considered [15]. It has been proposed that upon application of light-activated therapy, photogenerated free radicals are the crucial species responsible for the DNA cleavage [19–21]. A number of photoactive compounds require the contribution of a metal ion for the DNA cleavage event [22–26], therefore the biological activity of irradiated CPT was tested also in the presence of copper(II) ions [27–29]. The participation of iron in camptothecin-induced DNA cleavage is substantiated by the studies employing bleomycin–iron complex (alone or in con-

Abbreviations: CPT, camptothecin; DBNBS, 3,5-dibromo-4-nitrosobenzenesulfonic acid (sodium salt); DMPO, 5,5-dimethyl-1-pyrroline N-oxide; DMSO, dimethyl sulfoxide; DNA, deoxyribonucleic acid; DPPH, 1,1-diphenyl-2-picrylhydrazyl; EPR, electron paramagnetic resonance; ND, nitrosodurene, 2,3,5,6-tetramethyl-nitrosobenzene; PBS, phosphate-buffered saline; ROS, reactive oxygen species; TEMPOL, 4-hydroxy-2,2,6,6-tetramethylpiperidine N-oxyl; TMP, 4-hydroxy-2,2,6,6-tetramethylpiperidine; Topo I, topoisomerase I; SW, magnetic field sweep width

* Corresponding author. Tel.: +421 2 5932 5666; fax: +421 2 5292 6032.
E-mail address: vlasta.brezova@stuba.sk (V. Brezová).

1010-6030/$ – see front matter © 2006 Elsevier B.V. All rights reserved.
doi:10.1016/j.jphotochem.2006.06.001

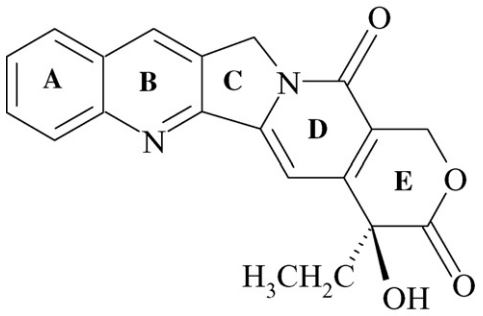

Scheme 1. Structure of camptothecin lactone form.

junction with NADPH as an additional reductant) which shown similar extent of DNA cleavage as camptothecin alone. In additon, besides the synergistic role of redox metals and anticancer drugs, iron acts as a stabilising metal to encapsulate CPT primarily in its active lactone form; it is of current interest to develop therapeutic assessment of CPT-loaded liposomes prepared using copper, iron and other metal ions [30].

The systematic investigation of electronic and fluorescence spectra of CPT in different solvents demonstrated that an increase in dielectric constant and proton-donating capacity of the solvent resulted in a hypsochromic shift of absorption maxima and slight bathochromic shift of fluorescence maxima [31–33]. Due to the rigid planar structure of CPT (containing an extended conjugation of four rings), camptothecin has a relatively high molar absorptivity [32,34] and fluorescence quantum yield ($\Phi_f \sim 0.3$–0.7, [31,32]). These data imply to suggest that the S_1 state of CTP is of $^1(\pi$–$\pi^*)$-type and there is a vibronic interaction between the $^1(\pi$–$\pi^*)$ and a close-lying higher energy $^1(n$–$\pi^*)$-state [32].

Recently, we have investigated the formation of radicals and singlet oxygen upon photoexcitation ($\lambda = 365$ nm) of CPT in DMSO by EPR spectroscopy [35] using spin trap agents DMPO and ND. Upon a continuous irradiation of CPT the generation of hydroxyl radicals was indicated via methyl radical originating from DMSO solvent. The photoinduced formation of singlet oxygen upon irradiation of CPT in aerated solutions was confirmed exploring its reaction with TMP [35,36]. However, upon irradiation of Cu(II):CPT = 1:1 in DMSO, the formation of methyl radical was suppressed and the generation of two new radical adducts, originating from camptothecin ring cleavage, was evidenced. The low temperature EPR spectra indicated in this system the proximity between Cu(II) ion and the 20-hydroxy group of the **E** ring of CPT [27,35]. Irradiating the argon-saturated Cu(II):CPT = 1:1 solutions in DMSO, the Cu(II) ions were reduced to Cu(I). The photoexcitation of Cu(II)–CPT in the presence of oxygen led to the generation of superoxide anion radical, identified as the $^{\bullet}$DMPO–O_2^- spin adduct [35,37–39].

Considering these data, our further investigations here are oriented now on iron, representing an essential element for a number of living organisms, as a component of molecules that undergo redox reactions or transport oxygen. Iron(III) is a spherically symmetrical tripositive cation classified as a hard Lewis acid by its high charge density. It forms most stable bonds with hard ligands such as charged hydroxamate oxygen atoms. In addition, chelators that bind iron(III) are capable of redox cycling, a property playing an important role in metallo-biology of cells. However, the redox reactions of iron can generate detrimental reactive oxygen species in the living cells [40,41]. Taking into account the above-mentioned properties of Fe(III), as well as the ability of irradiated CPT to produce free radical species, we undertook the spectroscopic study of Fe(III)–CPT systems.

2. Experimental details

2.1. Materials and equipments

Camptothecin (Sigma), DMSO (Fluka, stored over the molecular sieves), $Fe(NO_3)_3 \cdot 9H_2O$, 1,10-phenanthroline, $FeSO_4 \cdot 7H_2O$ (Lachema, Czech Republic) and H_3PO_4 (analytical grade, 85% Mikrochem, Slovak Republic) were used without further purification. The spin trapping agents ND and DBNBS were obtained from Aldrich.

UV/vis spectra were recorded using a UV/vis spectrometer PC 2000 (Sentronic, Germany) with a DH 2000 lamp, luminescence spectra with a Perkin-Elmer Luminescence spectrometer LS 50 B in a 1 cm quartz cell at 25 °C. Excitation and emission wavelengths of 365 and 430 nm, respectively, were applied in all experiments.

EPR spectra were measured at room temperature (295 K) and at 77 K (liquid nitrogen) using a cw-Bruker ER 200 D spectrometer, coupled with an Aspect 2000 computer, and a Bruker EMX spectrometer (both operating at X-band, with 100 kHz field modulation). As irradiation source served a HPA 400/30S lamp (400 W, Philips) equipped with a filter (Schott Glaswerke, Germany) selecting the wavelengths as specified in further text.

2.2. Sample preparation

All experiments were performed in DMSO solutions. DMSO is a strongly coordinating, aprotic polar solvent (dielectric constant $\varepsilon^{25} = 47$, [42]) and from a biological and medical point of view is suitable for this type of experiments (it is currently under study as a potential drug carrier) [43]. The CPT stock solutions prepared in DMSO avoid its spontaneous transformation to the carboxylate form (it remains in the lactone form), and prevent its self-aggregation [44].

2.3. EPR experiments

In the experiments at room temperature, the freshly prepared solutions were saturated at 101.3 kPa with argon, air or oxygen and then transferred into a quartz cell optimized for the Bruker cavity TM-110 (ER 4103 TM). In the experiments with nitrosodurene spin trapping agent the solutions were saturated with ND, due to its low solubility in DMSO solvent. The samples were irradiated directly in the microwave cavity by monochromatic light ($\lambda = 365$ nm; irradiance 8 mW cm^{-2}) and the EPR spectra were monitored in situ.

The EPR measurements in liquid nitrogen (77 K) were performed in the standard TE_{102} rectangular cavity using 4 mm o.d. quartz EPR tubes. However, the solutions here were irradiated ($\lambda = 365$ nm) outside of the EPR cavity, then immediately frozen in liquid nitrogen and after that EPR spectra were measured at low temperatures. A good quality of an amorphous structure was obtained by rapidly cooled sample in liquid nitrogen.

The individual components of spectra were simulated using the commercially available program SimFonia (Bruker) and program QPOW developed by Belford and Nilges [45]. The multi-component experimental EPR spectra of spin adducts were then fitted as the linear combinations of these individual simulations using a least-squares minimization procedure with the Scientist Program (MicroMath). The statistical parameters of calculation procedure (R^2, coefficient of determination and correlation) served for the determination of simulation quality, i.e. harmonization of experimental and simulated spectra. The relative concentration of the individual paramagnetic species was evaluated in the simulation from the contributions of their individual spectra to the experimental spectrum after double integration.

2.4. Photochemical experiments

Experiments were carried out at room temperature (295 K) under argon. The freshly prepared solutions were irradiated in quartz EPR flat cell with a focused light beam from a HPA source selecting the wavelength of 365 nm. The UV/vis spectra of the irradiated solutions were taken employing flat cell from EPR experiments.

2.5. Spectrophotometrical evidence of Fe(II) species in Fe(III)–CPT

The formation of Fe(II) ions upon irradiation was indicated spectrophotometrically using the Fe(II)-specific chelating agent 1,10-phenanthroline $[Fe(phen)_3]^{2+}$ ($\lambda_{max} = 512$ nm; $\varepsilon_{510} = 1.12 \times 10^4\ M^{-1}\ cm^{-1}$), which has redox stability towards oxygen. The interference of Fe(III) was eliminated adding phosphate ions able to bind Fe(III) into redox and thermodynamically stable, nearly colorless phosphate complexes [46,47].

After mixing the corresponding volumes of CPT and $Fe(NO_3)_3$ stock solutions to obtain for both 1 mM final concentration, the solution was set under argon atmosphere and transferred into EPR flat cell, irradiated (365 nm) during various exposure times (5, 10, 15, 20 and 30 min) at 295 K. After irradiation, the solutions (500 μl) were mixed under argon with excess of solid 1,10-phenanthroline and 25 μl of concentrated H_3PO_4. The mixture obtained was immediately transferred to the same EPR flat cell to record the UV/vis spectra. The reference solution consisted from the non-irradiated solution matching the composition as irradiated one. The concentrations of Fe(II) ions were evaluated using calibration plot from $FeSO_4$ solutions. An identical set of photochemical experiments was also performed with Fe(III):CPT = 1:1 but solutions were saturated with air.

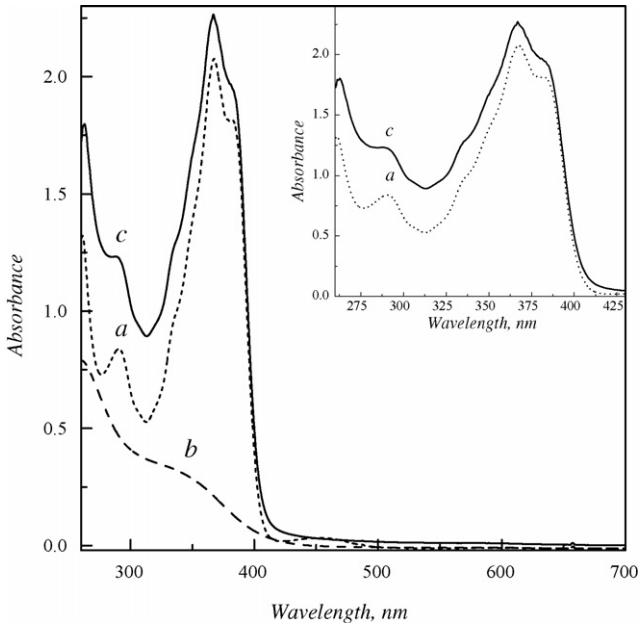

Fig. 1. UV/vis spectra of 1 mM DMSO solutions of: (a) CPT (dotted line), (b) $Fe(NO_3)_3$ (dashed line) and (c) Fe(III):CPT = 1:1 (solid line). Cell length 0.1 cm. (Inset) detail of (a) and (c) in the region 260–430 nm.

3. Results and discussion

3.1. UV/vis and fluorescence spectroscopy of non-irradiated CPT and Fe(III):CPT = 1:1

Fig. 1 presents the absorption UV/vis spectra of 1 mM DMSO solutions of (a) CPT, (b) $Fe(NO_3)_3$ and (c) Fe(III):CPT = 1:1. The absorption spectra of (a) and (c) exhibit absorption maxima at $\lambda^1_{abs} = 383$ nm (shoulder), $\lambda^2_{abs} = 368$ nm, $\lambda^3_{abs} = 335$ nm (shoulder) and $\lambda^4_{abs} = 290$ nm, in good agreement with data published by Nabiev et al. [44].

The UV/vis spectra of (a) CPT and (c) Fe(III):CPT = 1:1 are nearly identical; no additional charge-transfer bands were observed in the region over 500 nm. The spectrum of Fe(III):CPT = 1:1 can be evaluated as a simple linear combination of the corresponding $Fe(NO_3)_3$ and CPT spectra. Consequently, it can be assumed that the CPT does not bind to iron(III) in the inner coordination sphere. This observation is expected, as DMSO used is a strongly coordinating solvent [35].

Fig. 2 presents the emission and excitation fluorescence spectra of CPT and of Fe(III):CPT = 1:1 in DMSO solvent saturated with nitrogen. The fluorescence emission spectrum of CPT under these experimental conditions consists from only one wide band characterized by a fluorescence maximum at $\lambda_{max} = 429$ nm with Stokes shift $\Delta\lambda_{ST} = 46$ nm, and is independent of the excitation wavelength (Fig. 2). The addition of iron(III) ions in equimolar concentration (2.5 μM) to CPT causes a substantial drop of its fluorescence intensity ($I_L = 0.64 I^0_L$; Fig. 2) most likely due to interaction of CPT excited states with Fe(III) ions.

Previously, investigations of the fluorescence spectra of CPT in the presence of Co(II) ions (concentration range 0–0.12 M) in aqueous solution [31], or in the presence of iodide ions (concentration range 0–0.2 M) in PBS solution [32], provided evidence

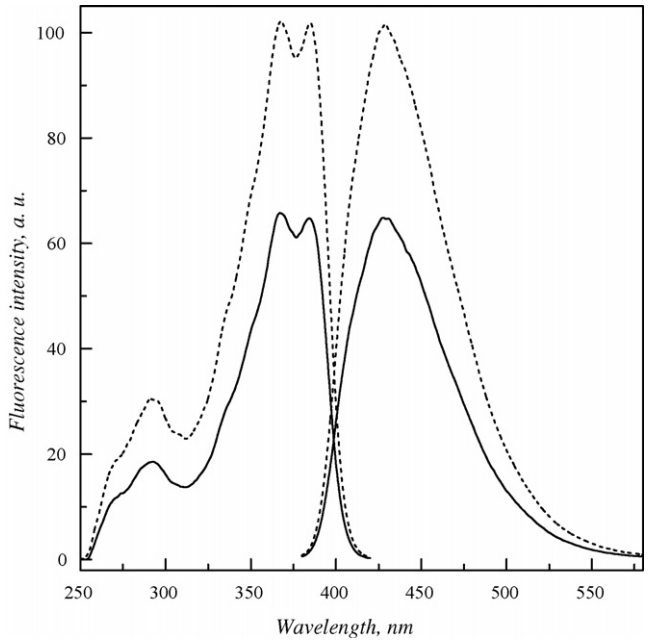

Fig. 2. Fluorescence (emission and excitation) spectra of 2.5 μM DMSO solutions of CPT (dotted line) and Fe(III):CPT = 1:1 (solid line) measured under nitrogen atmosphere. Excitation and emission wavelengths: 365 and 430 nm; cell length 1 cm.

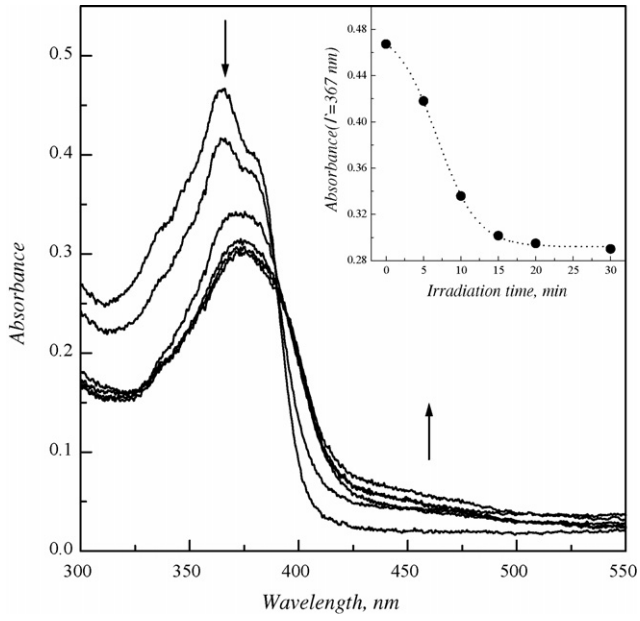

Fig. 3. UV/vis spectra of a 1 mM Fe(III)–CPT solution in DMSO irradiated (λ = 365 nm) during 0, 5, 10, 15, 20 and 30 min in a quartz EPR flat cell (length 0.02 cm) under argon. (Inset) absorbance decrease monitored at 367 nm.

that the CPT excited states were quenched by these ions and fluorescence emission was quenched at the diffusion controlled limit ($\sim 10^{10}$ M^{-1} s^{-1}) [31].

3.2. Photochemical experiments in Fe(III):CPT = 1:1 solutions

Our previous study of irradiated Cu(II):CPT = 1:1 system in DMSO solution evidenced the changes of UV/vis spectra of this complex upon irradiation, as well as reduction of Cu(II) to Cu(I) ions [35]. Consequently, we applied analogous set of experiments to Fe(III):CPT = 1:1 in DMSO solutions.

The changes in the UV/vis spectra upon irradiation (365 nm) of an argon-saturated 1 mM solution of Fe(III):CPT = 1:1 in DMSO shown in Fig. 3 reveals an exponential decrease in absorption maxima at 367 nm (inset in Fig. 3). A simultaneous absorbance increase observed in the region of 456 nm, probably arise from the photodecomposition of CPT via products with more extended π-electron systems [16–18,35].

To obtain an evidence of the above assumed reduction of Fe(III) to Fe(II) upon irradiation, the iron(II) ions were determined after irradiation by means of chelating agent 1,10-phenanthroline, which forms a colored Fe(II) complex absorbing at 512 nm [46,47]. Fig. 4 shows the time-course of visible spectra measured after irradiation of 1 mM Fe(III):CPT = 1:1 adding 1,10-phenanthroline, all carried out under inert atmosphere (Fig. 4a) and in the presence of air (Fig. 4b). The indicated reduction of Fe(III) to Fe(II) is nearly 100% after 30 min of irradiation in the argon-saturated systems (inset in Fig. 4a). However, the yield of Fe(II) in an analogous experiment under air is lower (75%; inset in Fig. 4b), due to presence of oxygen, which serves simultaneously as a very good acceptor of electrons.

3.3. EPR spectroscopy of non-irradiated and irradiated Fe(III)–CPT systems

3.3.1. Fe(III)–CPT

Iron(III) is a high spin paramagnetic ion ($3d^5$, $S = 5/2$). The Fe(III) ion is a ground state ^6S ($^6A_{1g}$ in the complexes) and is not split within an octahedral or even a lower symmetry ligand field [48]. In addition, there is no splitting by spin–orbital interaction. Then a single isotropic resonance line at $g \sim 2$ should always be observed. In fact, the low temperature (77 K) X-band EPR spectrum of Fe(III) in DMSO solutions represent only one very broad signal—as typically seen for Fe(III) [48,49]. However, after photoexcitation of CPT in the presence of iron(III) ions followed by immediate freezing in liquid nitrogen (77 K), we observe by EPR the generation of a new paramagnetic signal characterized by g-value of 2.0022, which could be attributed to carbon-centered radicals [35,50]. The appearance of this paramagnetic species confirms the photoinduced transformation of camptothecin via radical formation upon irradiation of the Fe(III)–CPT system. These radicals were investigated and analyzed in detail using the EPR spin trapping technique.

3.3.2. DBNBS and ND spin trapping agents

The EPR spin trapping technique enables to determine reactive short-lived free radicals adding them to spin trapping agent under the formation of more stable paramagnetic products (spin adducts). The adduct EPR spectrum brings information about the type of reactive radical trapped [37]. Two nitroso spin trapping agents, namely DBNBS and ND (Scheme 2), especially suit-

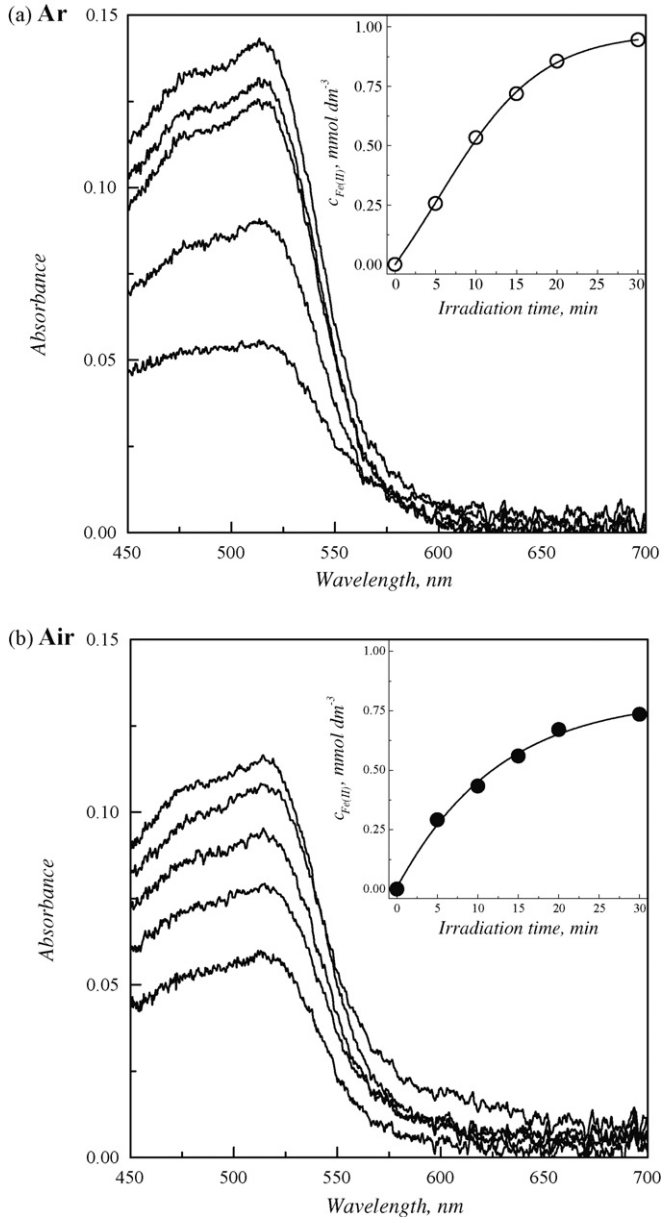

Fig. 4. Vis spectra of 1 mM Fe(III)–CPT DMSO solution irradiated (λ = 365 nm) during 0, 5, 10, 15, 20 and 30 min under: (a) argon and (b) air measured after addition of 1,10-phenanthroline (Fe(II)-specific chelator). The solutions were irradiated and measured in a quartz EPR flat cell of 0.02 cm). (Insets) evaluated Fe(II) concentration upon increased irradiation time.

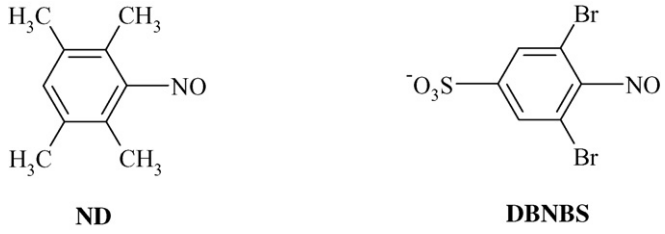

Scheme 2. Structures of ND and DBNBS spin trapping agents.

able for the identification of carbon-centered radicals were used [37]. The application of widely used DMPO as the spin trap was not possible here in systems containing Fe(III) ions and DMSO solvent, due to the formation of paramagnetic species even after mixing of individual solutions before irradiation, so the identification of photoinduced radical adducts is hardly possible.

In the blank experiments (mixing of ND or DBNBS solutions with Fe(III) or CPT without irradiation) no radicals were trapped, conforming suitability to use these agents in our experiments.

3.3.3. ND and CPT

The photoexcitation of argon-saturated 1 mM DMSO solution of CPT in the presence of ND yields an EPR signal characterized by hyperfine coupling constants of $a_N = 1.410$ mT and $a_H(3H) = 1.283$ mT and $g = 2.0055$ (Table 1). This spectrum is in a good accordance with $^{\bullet}$ND–CH_3 adduct [35,37]. The methyl radicals trapped are produced here from the DMSO solvent by its rapid reaction with hydroxyl radicals [51], probably originating from the lactone ring of CPT [35].

3.3.4. DBNBS and CPT

DBNBS spin trap in the argon-saturated 1 mM CPT solution brings evidence on the formation of four different carbon-centered adducts, their simulation parameters and relative concentrations are summarized in Table 2. Simulation of experimental EPR spectra (Table 2) measured after 3 min of continuous irradiation (λ = 365 nm) demonstrate that the major adduct (91%) characterized by hyperfine splittings of $a_N = 1.265$ mT, $a_H(2H) = 0.270$ mT, $a_H(2H^m) = 0.060$ mT and $g = 2.0060$ could be attributed to [$^{\bullet}$DBNBS–CR^1]$^-$. The relative concentrations of further spin adducts are significantly lower: [$^{\bullet}$DBNBS–CR^3]$^-$ (3%; $a_N = 1.265$ mT, $a_H(2H^m) = 0.060$ mT; $g = 2.0060$); [$^{\bullet}$DBNBS–CH_2R^2]$^-$ (4%; $a_N = 1.265$ mT, $a_H(2H) = 1.205$ mT, $a_H(2H^m) = 0.060$ mT; $g = 2.0060$) and methyl radical adduct (2%; $a_N = 1.341$ mT, $a_H(3H) = 1.210$ mT, $a_H(2H^m) = 0.068$ mT; $g = 2.0060$). We propose that the radical species [$^{\bullet}$DBNBS–CR^1]$^-$ and [$^{\bullet}$DBNBS–CR^3]$^-$ originate from the photoinduced destruction of lactone ring of camptothecin [37,52,53] and species [$^{\bullet}$DBNBS–CH_3]$^-$ and [$^{\bullet}$DBNBS–CH_2R^2]$^-$ are formed from DMSO solvent in the reactions with hydroxyl radicals producing $^{\bullet}CH_3$ and $^{\bullet}CH_2SOCH_3$ radicals [54].

3.3.5. ND and Fe(III):CPT = 1:1

The blank photochemical experiments (irradiating iron(III) ions in the presence of ND or DBNBS) showed only a negligible or no radical adduct formation. Consequently, these both spin traps are suitable for the application in the irradiated DMSO solutions containing Fe(III)–CPT.

The irradiation of argon-saturated DMSO solution of in the presence of ND results in the generation of three new, carbon-centered radicals (Table 1). The formation of $^{\bullet}$ND–CH_3 is completely suppressed. Simulation of experimental EPR spectra obtained after 10 min of continuous irradiation confirms as the most abundant $^{\bullet}$ND–CR^1 rad-

Table 1
Experimental (solid line) and simulated (dotted line) EPR spectra obtained after 10 min of a continuous irradiation (λ = 365 nm) of DMSO argon-saturated solutions containing: (a) 1 mM CPT and (b) 1 mM Fe(III)–CPT in the presence of ND spin trapping agent; c_r the relative radical concentrations in percentage and a_H, a_N and g are the simulation parameters (splitting constants and g-value)

EPR spectrum	c_r (%)	a_H, a_N (mT)	g-Value
(a) CPT	•ND-CH_3 100%	a_N = 1.410 a_H(3H) = 1.283	2.0055
SW = 10 mT			
(b) Fe(III)-CPT	•ND-CR^1 62%	a_N = 1.322	2.0058
	•ND-CR^2 36%	a_N = 1.515 a_H = 0.632	2.0055
	•ND-CR^3 2%	a_N = 1.515 a_H = 0.931	2.0055
SW = 7 mT			

ical (62%), represented with a three-line spectrum having $a_N = 1.322$ mT and $g = 2.0058$. The less abundant radical, •ND–CR^2 (36%), shows a six-line spectrum representing the interaction of the unpaired electron with one nitrogen and one hydrogen atom ($a_N = 1.515$ mT, $a_H = 0.632$ mT and $g = 2.0055$). These parameters correspond well to a spin adduct of the type •ND–CHR=CHR′ [37,55]. The third spin adduct, •ND–CHR^3, is found only in relative negligible concentration (2%; $a_N = 1.515$ mT, $a_H = 0.931$ mT; $g = 2.0055$). The radical species produced in this system upon irradiation most probably originate from decomposition of CPT molecules. The presence of Fe(III) ions enhanced the photoinduced transformation of camptothecin, and the concentration of radical adducts increased with Fe(III) concentration as demonstrated in Fig. 5.

3.3.6. DBNBS and Fe(III):CPT = 1:1

In under argon irradiated Fe(III):CPT = 1:1 system two radical adducts were observed in the presence DBNSB. EPR spectrum monitored after 3 min of continuous irradiation (Table 2) is compatible with two the carbon-centered radicals spin adducts, namely [•DBNBS–CR^1]$^-$ (76%; $a_N = 1.262$ mT, $a_H = 0.208$ mT; $g = 2.0060$) and [•DBNBS–CR^2]$^-$ (24%; $a_N = 1.255$ mT, $a_H = 0.728$ mT; $g = 2.0060$), most likely corresponding to the trapping of free radicals with structure •CHR=CHR′ [37,55].

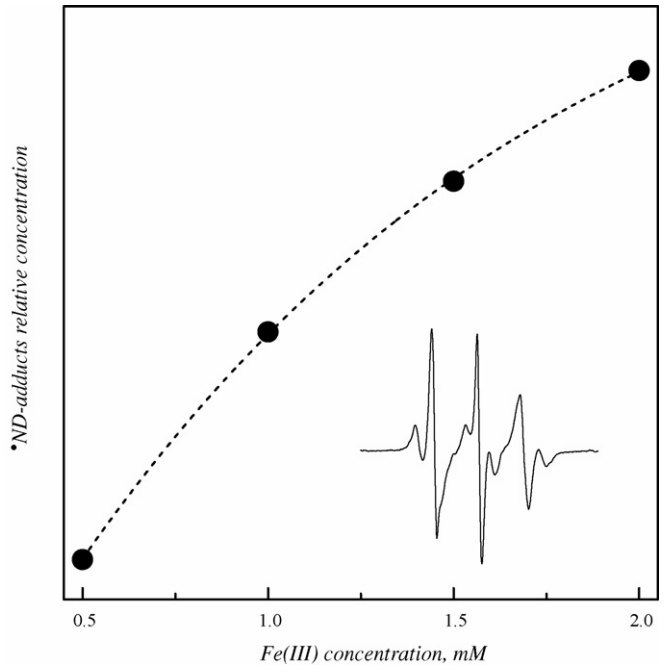

Fig. 5. Dependence of the relative •ND adduct concentrations upon the increasing Fe(III) concentrations added to 1 mM CPT solution, monitored after 10 min of a continuous irradiation (λ = 365 nm) under argon. (Inset) EPR spectrum with SW = 7 mT observed at ratio Fe(III):CPT = 2:1.

Table 2
Experimental (solid line) and simulated (dotted line) EPR spectra obtained after 3 min of continuous irradiation (λ = 365 nm) in DMSO argon-saturated solutions containing: (a) 1 mM CPT and (b) 1 mM Fe(III)–CPT in the presence of 0.2 mM DBNBS; c_r the relative radical concentrations in percentage and a_H, a_N and g are the simulation parameters (splitting constants and g-value)

EPR spectrum	c_r (%)	a_H, a_N (mT)	g-Value
(a) CPT	[•DBNBS-CR^1]$^-$ 91%	a_N = 1.265 a_H(2H) = 0.270 a_H(2H^m) = 0.060	2.0060
	[•DBNBS-CH$_2$R^2]$^-$ 4%	a_N = 1.265 a_H(2H) = 1.205 a_H(2H^m) = 0.060	2.0060
	[•DBNBS-CR^3]$^-$ 3%	a_N = 1.265 a_H(2H^m) = 0.060	2.0060
	[•DBNBS-CH$_3$]$^-$ 2%	a_N = 1.341 a_H(3H) = 1.210 a_H(2H^m) = 0.068	2.0060
SW = 8 mT			
(b) Fe(III)-CPT	[•DBNBS-CR^1]$^-$ 76%	a_N = 1.262 a_H = 0.208	2.0060
	[•DBNBS-CR^2]$^-$ 24%	a_N = 1.255 a_H = 0.728	2.0060
SW = 8 mT			

Fig. 6 shows the time-course of EPR spectra measured upon continuous irradiation of Fe(III):CPT = 1:1 in DMSO solution in the presence of DBNBS under: (a) argon, (b) air and (c) oxygen. The highest radical population was found under argon, lower one under air and practically no radicals were observed under oxygen. A decrease of relative adducts population with the prolonged irradiation is probably caused by the consecutive reactions of spin adducts. These results are well compatible with an assumption of a fast addition of molecular oxygen to the primary formed carbon-centered radicals converting then to peroxyl and alkoxyl radicals [54]. As the stability of adducts from oxygen-centered radical to ND and DBNBS spin traps is very low [35,56], this can explain the decreasing adduct populations with growing presence of oxygen in Fig. 6. Although we could not confirm here the formation of oxygen-centered adducts by DMPO, because of restriction caused with the presence of iron ions, it may be added that in similar experiments with Cu(II):CPT = 1:1 during photoexcitation of oxygen-saturated solutions in the presence of DMPO as a spin trap, we observed the generation of superoxide anion radicals [35].

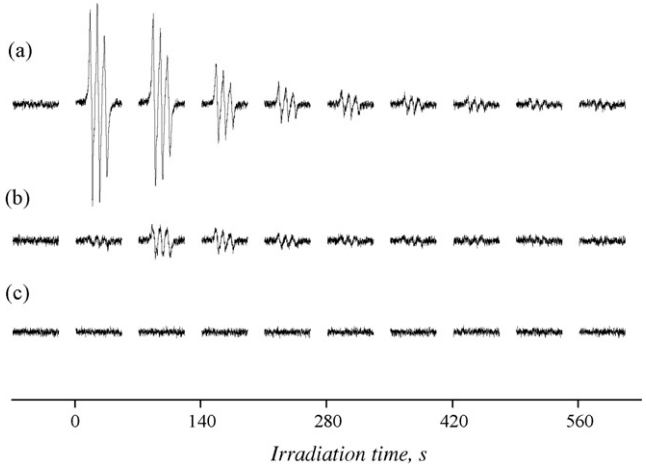

Fig. 6. Time-course of EPR spectra (SW = 8 mT) obtained upon continuous irradiation of 1 mM Fe(III):CPT = 1:1 in DMSO solutions in the presence of DBNBS spin trapping agent (c_{DBNBS} = 0.2 mM) under: (a) argon, (b) air and (c) oxygen atmosphere.

The excited species of a prospective phototherapeutic agent can undergo various reactions, among which electron-transfer and energy transfer processes are probably the most important [35,40,41]. CPT has been reported to be photoactive via a π–π^* photoexcitation [14–18,35]. The investigations of electron transfer processes in biochemical systems showed that, in most cases, a close contact between the donor and acceptor molecules is required for an efficient electron transfer, particularly in photoinduced electron transfer [41,57,58]. In our previous study of the Cu(II)–CPT system, the proximity between the Cu(II) ion and the CPT molecule has been found, and the mechanism of the

reactive radical species formation in the presence of copper(II) ions in irradiated CPT solution was suggested [35].

The investigations of photoinduced processes of Fe(III)–CPT system in DMSO solutions here demonstrate the reduction of Fe(III) to Fe(II) ions and a simultaneous radical species formation; where Fe(III) concentration increase enhances the yield of spin adducts (Fig. 5).

Two alternative mechanisms may be considered for the photoinduced electron transfer. The first assumes photoexcitation of Fe(III)–CPT (Eq. (1)) followed by the direct electron transfer to Fe(III) ions producing Fe(II) and cation radical of CPT (Eq. (2)). The presence of $CPT^{\bullet+}$ was confirmed previously in the buffered solution (pH 4) by transient absorption spectroscopy [59]. The second alternative assumes the generation of $\{Fe(III)\cdots CPT^{\bullet+}\}$ intermediates accompanied with a release of solvated electron (Eq. (3)) and its consecutive reaction with Fe(III) gives Fe(II) ions (Eq. (4)). This process of electron transfer is particularly efficient in DMSO, which can stabilize the cation radical of CPT (highly polar, aprotic solvent able to solvate strongly cations but only weakly anions). In both considered alternatives the generated $CPT^{\bullet+}$ (Eqs. (2) and (4)) is involved in the formation of radical intermediates (Eq. (5)), identified here using ND and DBNBS spin traps.

$$Fe(III) + CPT + h\nu \rightarrow \{Fe(III)\cdots CPT^{*}\} \quad (1)$$

$$\{Fe(III)\cdots CPT^{*}\} \rightarrow Fe(II) + CPT^{\bullet+} \quad (2)$$

$$\{Fe(III)\cdots CPT^{*}\} \rightarrow \{Fe(III)\cdots CPT^{\bullet+}\} + e_{(slov)}{}^{-} \quad (3)$$

$$\{Fe(III)\cdots CPT^{\bullet+}\} \rightarrow e_{(slov)}{}^{-} \rightarrow \{Fe(II)\cdots CPT^{\bullet+}\} \rightarrow Fe(II) + CPT^{\bullet+} \quad (4)$$

$$CPT^{\bullet+} \rightarrow \text{radical products} \quad (5)$$

4. Conclusions

The work was focused on the spectroscopic characterization of photoinitiated processes of Fe(III)–CPT in DMSO solvent applying EPR, UV/vis absorption and fluorescence spectroscopy. The results obtained confirm the participation of Fe(III) ions in the photoinitiated activation of camptothecin accompanied with the formation of reactive radical species.

Acknowledgments

This work was supported by the Science and Technology Assistance Agency under the contract no. APVT-20-005702 and Slovak Grant Agency (Projects VEGA 1/0053/03, VEGA 1/3579/06 and VEGA 1/2450/05). We thank Professor A. Horváth (Veszprém University, Veszprém, Hungary) for fruitful discussion and for the possibility to measure luminescence spectra and the referee for valuable comments.

References

[1] T.G. Burke, A.E. Staubus, A.K. Mishra, J. Am. Chem. Soc. 114 (1992) 8318–8319.
[2] T.G. Burke, A.K. Mishra, M.C. Wani, M.E. Wall, Biochemistry 32 (1993) 5352–5364.
[3] X.Y. Wang, X.A. Zou, S.M. Hecht, Biochemistry 38 (1999) 4374–4381.
[4] X.Y. Wang, L.K. Wang, W.D. Kingsbury, R.K. Johnson, S.M. Hecht, Biochemistry 37 (1998) 9399–9408.
[5] M. Potmesil, H. Pinedo (Eds.), Camptothecins: New Anticancer Agents, CRC Press, Boca Raton, FL, 1995.
[6] Y.-H. Hsiang, R. Hertzberg, S. Hecht, L.F. Liu, J. Biol. Chem. 260 (1985) 14873–14878.
[7] M.R. Mattern, S.-M. Mong, H.F. Bartus, C.K. Mirabelli, S.T. Crooke, R.K. Johnson, Cancer Res. 47 (1987) 1793–1798.
[8] Y.-H. Hsiang, L.F. Liu, Cancer Res. 48 (1988) 1722–1726.
[9] S.M. Hecht, Curr. Med. Chem.—Anti-Cancer Agents 5 (2005) 353–362.
[10] X.S. Xiao, M. Cushman, J. Org. Chem. 70 (2005) 9584–9587.
[11] C.H. Takimoto, J. Wright, S.G. Arbuck, Biochim. Biophys. Acta 1400 (1998) 107–119.
[12] D.J. Adams, M.W. Da Silva, J.L. Flowers, G. Kohlhagen, Y. Pommier, O.M. Colvin, G. Manikumar, M.C. Wani, Cancer Chemother. Pharmacol. 57 (2006) 135–144.
[13] D.J. Adams, M.L. Wahl, J.L. Flowers, B. Sen, O.M. Colvin, M.W. Dewhirst, G. Manikumar, M.C. Wani, Cancer Chemother. Pharmacol. 57 (2006) 145–154.
[14] J.W. Lown, H.H. Chen, Biochem. Pharmacol. 29 (1980) 905–915.
[15] F. Leteurtre, M. Fesen, G. Kohlhagen, K.W. Kohn, Y. Pommier, Biochemistry 32 (1993) 8955–8962.
[16] K. Akimoto, A. Kawai, K. Ohya, J. Chromatogr. A 734 (1996) 401–404.
[17] H.M. Dodds, J. Robert, L.P. Rivory, J. Pharm. Biomed. Anal. 17 (1998) 785–792.
[18] H.M. Dodds, D.J. Craik, L.P. Rivory, J. Pharm. Sci. 86 (1997) 1410–1416.
[19] A. Natrajan, S.M. Hecht, J. Org. Chem. 56 (1991) 5239–5241.
[20] S.A. Kane, H. Sasaki, S.M. Hecht, J. Am. Chem. Soc. 117 (1995) 9107–9118.
[21] H. Falk, Angew. Chem. Int. Ed. Engl. 38 (1999) 3117–3136.
[22] D.R. McMillin, K.M. McNett, Chem. Rev. 98 (1998) 1201–1219.
[23] P. Lugo-Ponce, D.R. McMillin, Coord. Chem. Rev. 208 (2000) 169–191.
[24] Z.Z. Ou, J.R. Chen, X.S. Wang, B.W. Zhang, Y. Cao, Chem. Lett. 2 (2002) 206–207.
[25] J. Onuki, P.C. Teixeira, M.H.G. Medeiros, D. Dornemann, T. Douki, J. Cadet, P. Di Mascio, Cell. Mol. Biol. 48 (2002) 17–26.
[26] X. Wang, K.A. Henningfeld, S.M. Hecht, Biochemistry 37 (1998) 2691–2700.
[27] J. Kuwahara, T. Suzuki, K. Funakoshi, Y. Sugiura, Biochemistry 25 (1986) 1216–1221.
[28] J. Kuwahara, T. Suzuki, Y. Suguira, Nucleic Acids Symp. Ser. 16 (1985) 201–204.
[29] R.P. Hertzberg, M.J. Caranfa, S.M. Hecht, Biochemistry 28 (1989) 4629–4638.
[30] J.W. Lown, H.H. Chen, J.A. Plambeck, Chem. Biol. Interact. 35 (1981) 55–70.
[31] Y. Posokhov, H. Biner, S. Içli, J. Photochem. Photobiol. A: Chem. 158 (2003) 13–20.
[32] J. Dey, I.M. Warner, J. Lumin. 71 (1997) 105–114.
[33] J. Dey, I.M. Warner, J. Photochem. Photobiol. A: Chem. 101 (1996) 21–27.
[34] D. Chauvier, I. Chourpa, M. Maizieres, J.-F. Riou, M. Dauchez, A.J.P. Alix, M. Manfait, J. Mol. Struct. 651 (2003) 55–56.
[35] V. Brezová, M. Valko, M. Breza, H. Morris, J. Telser, D. Dvoranová, K. Kaiserová, L. Varečka, M. Mazúr, D. Leibfritz, J. Phys. Chem. B 107 (2003) 2415–2425.
[36] L.Y. Zang, F.J.G.M. van Kuijk, B.R. Misra, H.P. Misra, Biochem. Mol. Biol. Int. 37 (1995) 283–293.
[37] A.S.W. Li, K.B. Cummings, H.P. Roethling, G.R. Buettner, C.F. Chignell, J. Magn. Reson. 79 (1988) 140 (The database is available through internet at: http://epr.niehs.nih.gov).
[38] J.R. Harbour, M.L. Hair, J. Phys. Chem. 82 (1978) 1397–1399.
[39] H. Noda, K. Oikawa, H. Ohya-Nishiguchi, H. Kamada, Bull. Chem. Soc. Jpn. 66 (1993) 3542–3547.
[40] M. Valko, M. Izakovič, M. Mazúr, C.J. Rhodes, J. Telser, Mol. Cell. Biochem. 266 (2004) 37–56.

[41] K. Szacilowski, W. Macyk, A. Drzewiecka-Matuszek, M. Brindell, G. Stochel, Chem. Rev. 105 (2005) 2647–2694.
[42] http://www.organicdivision.org/organic_solvents.html.
[43] K.V. Balakin, Curr. Drug Discovery (2003) 27–32.
[44] I. Nabiev, F. Fleury, I. Kudelina, Y. Pommier, F. Charton, J.-F. Riou, A.J.P. Alix, M. Manfait, Biochem. Pharmacol. 55 (1998) 1163–1174.
[45] R.L. Belford, M.J. Nilges, Computer simulation of powder spectra, in: EPR Symposium, 21st Rocky Mountain Conference, Denver, CO, August 1979.
[46] J. Šima, Pol. J. Chem. 66 (1992) 963–967.
[47] F. Renz, W. Linert, P. Fleischhauer, R. Klement, M. Mazúr, J. Šima, R. Boča, in: G. Ondrejovič, A. Sirota (Eds.), Current Trends in Coordinated Chemistry, Slovak Technical University Press, Bratislava, 1995, pp. 303–308.
[48] W. Gordy, Theory and Applications of Electron Spin Resonance, Wiley, 1980.
[49] B.A. Goodman, J.B. Raynor, in: H.J. Enchens, A.G. Sharpe (Eds.), Electron Spin Resonance of Transition Metal Complexes in Advanced Inorganic Radiochemistry, Academic Press, New York, 1970, pp. 135–362.
[50] O. Madelung (Ed.), Landolt-Börnstein Numerical Data and Functional Relationships in Science and Technology, New Series, Group II: Atomic and Molecular Physics, vol. 17, Magnetic Properties of Free Radicals, subvolume c: Conjugated Carbon-Centered and Nitrogen Radicals, Springer, Berlin, 1987.
[51] J.R. Woodward, T.-S. Lin, Y. Sakaguchi, J.H. Hayashi, J. Phys. Chem. A 104 (2000) 557–561.
[52] C.L. Hawkins, M.J. Davies, Free Radic. Biol. Med. 21 (1996) 275–290.
[53] C.L. Hawkins, M.J. Davies, Free Radic. Biol. Med. 24 (1998) 1396–1410.
[54] http://www.medicine.uiowa.edu/firrb/SRFRS/SRFRS-papers/SFRS-2001-BuettnerG.pdf.
[55] A. Staško, P. Rapta, V. Brezová, O. Nuyken, R. Vogel, Tetrahedron 49 (1993) 10917–10924.
[56] V. Brezová, P. Tarábek, D. Dvoranová, A. Staško, S. Biskupič, J. Photochem. Photobiol. A: Chem. 155 (2003) 179–198.
[57] C. Wan, T. Fiebig, S.O. Kelley, C.R. Treadway, J.K. Barton, A.H. Zewail, Proc. Natl. Acad. Sci. U.S.A. 96 (1999) 6014–6019.
[58] G. Jones II, X. Zhou, V.I. Vullev, Photochem. Photobiol. Sci. 2 (2003) 1080–1087.
[59] K. Steenkeste, E. Guiot, F. Tfibel, P.P. Ernot, F. Mérola, P. Georges, M.P. Fontaine-Aupart, Chem. Phys. 275 (2002) 93–108.